Published in final edited form as:
Biomaterials. 2007 March ; 28(8): 1503–1514.

Dynamics of smooth muscle cell deadhesion from thermosensitive hydroxybutyl chitosan

Beiyi Chen[a], **Jiyoung Dang**[b], **Tuan Lin Tan**[c], **Ning Fang**[a], **Wei Ning Chen**[a], **Kam W. Leong**[d], and **Vincent Chan**[a,*]

a *Center of Biotechnology, School of Chemical and Biomedical Engineering, Nanyang Technological University, Singapore 639798, Singapore*

b *Department of Biomedical Engineering, Johns Hopkins University, 720 Rutland Avenue/Ross 720, Baltimore, MD 21205, USA*

c *School of Biological Sciences, Nanyang Technological University, Singapore 637551, Singapore*

d *Biomedical Engineering Department, Duke University, Room 136 Hudson Hall, Box 90281, Durham, NC 27708-0281, USA*

Abstract

Thermoresponsive polymer (TRP) enables the enzyme-free harvesting of cells through an acute increase in surface hydrophilicity of TRP across its lower critical solution temperature (LCST), rendering feasible the generation of polymer-free cell sheets for regenerative medicine applications. To date, the intricate mechanisms of cell deadhesion/detachment on TRP surface remain obscure. Elucidation of such biophysical responses would be valuable for the cell sheet technology. In this study, integrative biophysical techniques are applied to probe the thermal-induced deadhesion kinetics of smooth muscle cell (SMC) on thermoresponsive hydroxybutyl chitosan (HBC29) against different periods of pre-culture time at 37 °C. Atomic force microscopy demonstrates that both the surface topography and mechanical property of HBC29 film in water are acutely modulated across its LCST. Firstly, cells show negligible changes in adhesion contact area during low-temperature incubation on unmodified tissue culture polystyrene (TCPS). Secondly, the recession of adhesion contact and retraction of cell body for cells with different pre-culture times are triggered by HBC29 coating on TCPS. Interestingly, the initial rate of reduction in the normalized adhesion contact area of SMC is negatively correlated with the pre-culture time. Thirdly, the degree of cell deformation and average adhesion energy are reducing functions of time only for SMCs with the lowest pre-culture time. In contrast, adhesion energy per cell is a reducing function of time irrespective of the change of pre-culture time. Lastly, the temporal dynamics of cytoskeleton organization and β-actin/smoothelin-B mRNA expression for SMCs is strongly dependent on the pre-culture time. Overall, this study demonstrates that the thermal-induced deadhesion of SMC on TRP is characterized by the evolution of its contractile phenotypes.

Keywords

Deadhesion kinetics; Chitosan derivative; Cell biophysics; Cytoskeleton dynamics

*Corresponding author. E-mail address: mvchan@ntu.edu.sg (V. Chan).

1. Introduction

Thermoresponsive polymers (TRP) as an emerging class of biomaterials have received much attention from the biomedical communities. The potential of TRP stems from its dramatic physical responses against the change of external temperature [1]. The thermal sensitivity of TRP is commonly characterized by the lower critical solution temperature (LCST). Specifically, the significant change in hydrophobicity of TRP above LCST induces the intermolecular aggregation of TRP. The acute switching between the hydrophobic and hydrophilic states of TRP against the change of temperature creates interesting opportunities for scaffolding design in tissue engineering. Confluent cell layer can be detached and released into the culture medium from TRP when temperature drops below LCST [2]. The use of TRP eliminates the use of proteolytic enzymes like dispase or physical scraping for recovering cells from tissue culture dish. Both conventional methods of cell/tissue recovery as mentioned above lead to the disruption of intercellular junctions and alteration of native tissue organization. During the past decade, Okano and coworkers have pioneered the chemical grafting of poly (*N*-isopropylacrylamide) PIPAAm onto tissue culture polystyrene (TCPS) for the enzyme-free recovery of confluent cell sheet of keratinocyte, Madin–Darby canine kidney (MDCK) cell, and hepatocyte [3].

The physiochemical properties of TRP as well as cell type are known to influence the time taken for complete detachment of cell sheet. It has been shown that the time of cell sheet detachment from various derivatives of PIPAAm ranges from 3 min to 24 h when the temperature is rapidly cooled below LCST [4]. Despite the rapid development of TRP in cell/tissue recovery, there is a lack of quantitative correlation between the cell–substrate interaction, cell mechanics, physiochemical properties of TRP, and ultimately cellular functions during the course of cell recovery. In particular, the kinetics of cell deadhesion and detachment during the thermal-induced transformation of TRP is not known. Our group has been actively engaged in the development of integrated biophysical techniques to elucidate the adhesion contact dynamics of several cell types on biomaterials during the initial phase of cell seeding [5]. We hypothesize that this biophysical approach may also be beneficial for probing the cell deadhesion/detachment kinetics towards temperature drop on TRP surface.

Hydroxybutyl chitosan (HBC), a promising TRP, which is synthesized by conjugation of hydroxybutyl groups to chitosan is used herein. Recently, HBC29 with a LCST of 29 °C has been developed for therapeutic applications related to injectable delivery of human mesenchymal stem cells [6]. In this study, the deadhesion kinetics of smooth muscle cell (SMC) from HBC29 is probed with confocal reflectance interference contrast microscopy (C-RICM) in conjunction with phase contact microscopy. SMC is chosen as our model system because the regeneration and recovery of SMC cell/tissue from TRP is potentially important for the development of artificial blood vessel [7]. Moreover, A7r5 SMC cell exhibiting the characteristic phenotypes of SMC, namely the morphologic plasticity in converting from contractile cells to highly motile proliferative cells, is an ideal platform for testing specific biological responses. Specifically, we aim to elucidate the biophysical mechanisms of cell deadhesion on HBC29 against the change of pre-culture time at 37 °C before subjected to a temperature drop. Several biophysical parameters derived from the temporal trends of normalized contact area and degree of cell deformation are found to be dependent on the pre-culture time. Also, the cytoskeleton structure of SMC and mRNA expressions of SMC markers during the course of cell deadhesion are determined. Interestingly, the average adhesion energy and adhesion energy per cell of SMCs are only found as reducing functions of time in SMCs with the lowest pre-culture time. Our results as described herein will provide a foundation for developing new design principles in cell sheet engineering for cells/tissues regeneration with the desirable phenotypes.

2. Materials and methods

2.1. Materials

HBC29 was obtained from Dainichiseika Color & Chemicals Mfg. Co., Ltd. (Tokyo, Japan). High glucose Dulbecco's modified eagle's medium (DMEM), fetal bovine serum (FBS), streptomycin, penicillin, 10 × tripson-EDTA (0.5%), 10 × PBS (pH = 7.4) were purchased from Gibco (Singapore). Acetic acid, formaldehyde, triton X-100 and FITC-phalloidin were purchased from Sigma Pvt. Ltd. (Singapore). Highly purified 18.2 MΩ water was obtained from water purification system (Sartorius, Germany).

2.2. Thermoresponsive polymer coating

HBC29 was subjected to a mild purification as described previously [6]. The HBC29 coating on TCPS surface was prepared with 1% polymer solution. In brief, HBC29 was dissolved into 1% acetic acid in distilled water and stirred overnight at room temperature. After centrifugation at 11,400 rpm for 30 min, the supernatant (transparent solution) was collected. 500 μL of above solution was transferred onto TCPS dishes and dried at 37 °C for 2 days. The coating was then washed three times with 1 × PBS at 37 °C. The amount of coated HBC29 was around 130 μg/cm^2.

2.3. Contact angle measurement

Static contact angle measurements were conducted for HBC29 surface using a Krüss G10 instrument (Germany) and 18.2 MΩ water as the probe liquid. For consistency, contact angle measurements were taken at exactly 60 s after placement of a water droplet on the surface, and reported values represent the average and 95% confidence intervals obtained using at least three 20 μL droplets on at least three surfaces.

2.4. Atomic force microscopy

A MFP-3D atomic force microscope (Asylum Research, CA, USA) was applied in all measurements, which were carried with contact mode in deionized water. The cantilever with a spring constant of 0.32 N/m and a scanning rate of 1 Hz were used in all experiments. HBC29 film was coated onto a 35-mm round cover glass according to procedures as mentioned above. A temperature-controlling fluid cell was applied to control the temperature of the liquid and immersed polymer film. Each AFM topographic image is a representative data of at least three samples and is highly reproducible under the same procedures of sample preparation. The spring constant of each AFM cantilever used in this study was calculated with the built-in thermal noise method in the MFP-3D software. With the detected cantilever sensitivity and spring constant, the preset tip deflection (set point) value corresponding to the force of cantilever exerted on the surface can then be calculated.

2.5. Cell culture

A7r5 SMC (American Type Culture Collection (ATCC), Catalog #: CRL 1444) originally derived from embryonic rat aorta exhibiting the typical phenotypes of adult smooth muscle were cultured in high-glucose DMEM medium supplemented with 10% FBS, 5 mg/ml penicillin and 5 mg/ml streptomycin. Cell cultures were maintained at 37 °C under a humidified atmosphere of 5% CO_2 in air. The medium was changed every 2 days, and the cells were passaged at least once a week. Cells were detached from the culture flask by the addition of a 1:10, 0.5% 5.3 mM trypsin-EDTA solution in phosphate-buffered saline (PBS).

Before each experiment, the HBC29-coated TCPS were maintained above LCST (at 37 °C) in order to keep the surface hydrophobic. Then A7r5 cells at a density of 5200 cell/cm^2 were plated onto HBC29-coated TCPS at 37 °C. After 3, 9, or 24 h of seeding on the HBC29 surface,

the samples were immediately transferred to an online CO_2 incubator at 18 °C under a humidified atmosphere of 5% CO_2 in air for biophysical measurements.

2.6. Confocal reflection interference contrast microscopy

The system is based on a laser scanning confocal microscope (Pascal 5, Carl Zeiss, Germany) and is integrated with an online CO_2 incubator (Carl Zeiss, Germany). The illumination source is an argon ion laser with a maximum power of 1 mW and excitation wavelength of 488 nm; 20 × objective (NA: 1.25) was used in this study. The strong contact zone of the adhering cells appears as dark region on the image. Simultaneously, a transmitted light analyzer (Carl Zeiss, Germany) attached to the confocal microscope is used for performing phase contrast microscopy of the adherent cells.

In order to monitor the deadhesion/detachment dynamics of SMC from HBC29 below LCST, a series of C-RICM images on a region of each sample was taken against time of incubation at 18 °C. The image analysis was performed with ZSM 5 software (Carl Zeiss, Germany). The contact area of each cell was measured by drawing a region of interest with a PC mouse based on the criteria of the dark region (representing strong adhesion contact). At the same time, the projected area of the adherent cells was determined from the phase contrast image. Therefore, the average radius of contact area a and projected area R of each cell was determined by C-RICM and phase contrast microscopy, respectively. At each time point, the average value of a and R was measured from 100 cells on at least four identical samples. Another biophysical parameter, normalized adhesion contact area was defined as the ratio of adhesion contact area at any time during cell deadhesion (A) and adhesion contact area immediately after the temperature reduction from 37 to 18 °C (A_0). Degree of deformation for each cell was defined as the ratio a/R [8].

2.7. Immunostaining and fluorescence microscopy

The cells at the different time points during cell deadhesion from HBC 29 surface were stained with FITC-phalloidin for actin filament labeling. In brief, SMCs were washed with cold PBS and fixed with 3% formaldehyde in 1 × PBS at room temperature for 10 min. The cells were permeabilized with 0.2 % triton X-100 in PBS for 10 min at room temperature following by a wash with 1 × PBS and blocking with 10% FBS and 0.1% Triton for another 10 min. For probing the structure of cytoskeleton, the fixed and permeabilized SMCs were incubated with fluorescein isothiocyanate-phalloidin (FITC-phalloidin) in 5% BSA for 1 h. After drying overnight, the cells were observed with fluorescence microscopy.

Fluorescence images of SMC immunostained with FITC-phalloidin were measured by confocal microscopy (Pascal 5, Carl Zeiss, Germany) fitted with a 20 × oil immersion objective, an argon-ion laser as the excitation source (488 nm), at a resolution of 1024 × 1024 pixels with the slow scan speed. Excitation light was set at 488 nm and fluorescence emission between 505 and 530 nm was recorded.

2.8. Reverse transcript-polymerase chain reaction

A7r5 SMCs were pre-cultured on HBC29 surface for 3 or 24 h, respectively. After pre-culture, the cells were then detached with 0.05% typsin-EDTA after incubation at 18 °C for 0, 30, or 60 min. Each batch of cells was collected and the total mRNA was extracted by RNeasy Mini Kit (Qiagen, Singapore) according to the recommended protocol. One microgram of the total mRNA was used for amplification using onestep Titanium RT-PCR Kit (Clontech). The mRNA was reverse-transcripted (RT) to cDNA at 50 °C for 1 h, and then the cDNA was denaturated at 94 °C for 5 min. Fifteen polymerase chain reaction (PCR) cycles consisted of 30 s denaturation at 94 °C, 30 s annealing at 65 °C, and 1 min extension at 68 °C for β-actin and 22 PCR cycles with the same reaction conditions for smoothelin-B. Primers specific for

β-actin were 5′-GTG GGC CGC TCT AGG CAC CAA-3′ (sense) and 5′-CTC TTT GAT GTC ACG CAC GAT TTC-3′ (antisense). And primers specific for smoothelin-B were 5′-GCT GGC ATC CGC CGA GTG-3′ (sense) and 5′-GCA CCT TAC CAG GGT CCA ATGT-3′ (antisense). Upon completion of reaction, 5 μL of the DNA products were electrophoresed on 1.5% agarose gel for 20 min at 100 V. DNA was stained with ethidium bromide (Sigma, Singapore), visualized under UV light and imaged by ChemDot (BioRad, USA).

2.9. Data analysis

The details of the contact mechanics model of adherent cells have been previously described [8]. Briefly, the equilibrium geometry of a cell adhering on a non-deformable substrate is modeled as a truncated sphere with a mid-plane radius *R*. The degree of deformation, $\sin\theta = (a/R) = \alpha$ is an experimentally measurable parameter where *R* and *a* are measured by C-RICM and phase contrast microscopy, respectively. The cell wall is under a uniform equibiaxial stress, $\sigma = T\varepsilon$. *T* is the stress equivalent and is equal to $Eh/(1-\nu)$ in a linear system under small strain, where *E*, *h* and *ν* are the elastic modulus, membrane thickness and Poisson's ratio, respectively. The average biaxial strain, *ε*, is directly calculated from *R* and *a* as follows:

$$\varepsilon = \frac{1}{2}\left[\frac{2+2(1-\alpha^2)^{1/2}}{4/R_a^2-\alpha^2}-1\right], \tag{1}$$

where

$$R_a = \frac{1}{16}\left[a^4+\frac{a^8}{f(a)}+f(a)\right]$$

and

$$f(a) = 2048 + 128a^6 + a^{12} + 16\sqrt{16384 + 2048a^6 + 80a^{12} + a^{18}}.$$

In the absence of external force, the cell spontaneously adjusts its distance of approach towards the substrate until equilibrium is achieved. It has been shown earlier that the adhesion energy, *W*, is as follows:

$$W = (1-\mathrm{Cos}\theta)C\varepsilon + C\varepsilon^2. \tag{2}$$

By taking a square root in the ratio of projected area (from phase contrast microscope) and adhesion contact area (from C-RICM), *a*/*R* is determined and *W* can be found by Eqs. (1) and (2). For the case of elliptical cell shape, *a*/*R* represents the ratio of the root mean square radius for adhesion contact $(\sqrt{a\times b})$ and root mean square radius of projected area $(\sqrt{R_1\times R_2})$, where *a* (R_1) and *b* (R_2) is the semi-major axis and semi-minor axis of the elliptical adhesion contact (projected shape), respectively. Thus *a*/*R* of an ellipse as mentioned above remains useful for comparing the size of adhesion contact with that of projected area. Despite the presence of elliptical cell shape during the early stage of cell deadhesion, our approach in quantifying the extent of adhesion contact formation against the projected cell area as mentioned above remains valid (K. T. Wan, personal communication). From Matsumoto's study, elastic modulus *E* of rat thoracic aortic SMCs is 9.3±2.8 KPa [9].

3. Results and discussion

In order to elucidate the effect of thermal transition of TRP (coated on TCPS) on the biophysical dynamics of adherent cells, we need to investigate the behavior of seeded cells on unmodified TCPS during a temperature drop across LCST. Fig. 1A shows the real-time phase contrast images and C-RICM images of a typical SMC (pre-cultured for 3 h at 37 °C and 5% CO_2) on

unmodified TCPS surfaces after 2 min and 15 h of incubation at 18 °C and 5% CO_2. From the phase contrast image, it is demonstrated that the cell adopts an elongated morphology after seeding on TCPS for 3 h at the physiological temperature. From C-RICM image, it is shown that strong adhesion contact (dark region) is formed between the cell and TCPS surface. Also, the projected area and adhesion contact area is 479.8 and 356.0 μm^2, respectively, after 2 min of 18 °C incubation. Based on the geometry of adherent cell, the adhesion contact area never exceeds the projected cell area. Interestingly, the cell still maintains its elongated morphology despite its subjection to 15 h incubation at 18 °C. Moreover, the projected area of cell slightly increases from 479.8 to 499.6 μm^2 from 2 min to 15 h after low-temperature incubation. In parallel, the adhesion contact zone slightly grows from 356 to 360.0 μm^2 during the same period. The result demonstrates that a temperature drop alone is not sufficient to trigger SMC deadhesion/detachment from unmodified TCPS surface after strong adhesion contact has been established during 3 h of pre-culture at 37 °C.

C-RICM has been proven as an effective tool for probing the adhesion contact dynamics of mammalian cells on biomaterials during the initial stage of cell seeding [13]. It is interesting to elucidate the effect of pre-culture time at physiological temperature on the biophysical responses of SMC during low-temperature incubation. Fig. 1B shows the real-time phase contrast images and C-RICM images of a typical SMC (pre-cultured for 24 h at 37°C and 5% CO_2) on unmodified TCPS surfaces after 2 min and 15 h of incubation at 18 °C and 5% CO_2. The cell initially adopts a more elongated morphology after 24 h pre-culture in comparison to that of cell after 3 h pre-culture. After 15 h, the phase contrast image indicates that the middle part of cell body (arrowhead) significantly contracts through the formation of longer lamellipodium. During the same period, C-RICM shows that the adhesion contact area recesses within the same region of cell contraction. Specifically, the projected area and adhesion contact area are reduced from 985.3 to 715.2 μm^2 (by 27%) and 721.0 to 637.8 μm^2 (by 11.5%), respectively, from 2 min to 15 h at 18 °C. In comparison with the cell at lower pre-culture time of 3 h, the result indicates that the prolonged culture at 37 °C leads to the higher % reduction in projected area and adhesion contact area during low-temperature incubation. Interestingly, the cell remains strongly adhered on TCPS as shown by the moderate reduction in adhesion contact area. Our result is supported by a recent study, which demonstrated that the viability, expansion and phenotype of peripheral blood lymphocytes are unaltered after low-temperature incubation [10]. The cell contraction is likely caused by the sub-optimal conditions for cell culture at 18 °C. In the absence of TRP, there is no significant thermal-induced deadhesion of cell on untreated TCPS for extended period, which is significantly longer than that in our cell deadhesion assay on TRP.

The interfacial properties of TRP film directly tune the cellular responses of adherent cell during thermal transition across LCST. Fig. 2 shows AFM topographic images of HBC29 film immersed in pure water at 37 and 18 °C. Above LCST, the polymer surface appears to be rough and is filled with small agglomerates with different height. The result is likely caused by the increase of hydrophobicity of the polymer chain and the subsequent dewetting of the polymer film. From the representative force curve at 37 °C under water (red spot on topographic image), the presence of a jump-in event (escape transition) at 108±12 nm (n = 10) from the polymer surface during the retraction of AFM tip indicates that there is a manifestation of adhesion force between the AFM tip and polymer film. Similar trend of force curve has been previously reported in poly-(butadiene)-*b*-poly(ethylene oxide) film supported on glass under aqueous medium [11]. Below LCST (18 °C), the AFM image indicates that the polymer surface is significantly smoother than that at 37 °C. The transformation of surface topography from 37 to 18 °C is supported by the significant reduction of root-mean-square roughness from 2.52 to 0.08 nm. At the same time, the representative force curve at 18 °C (red spot on topographic image) under water shows that the jump-in during the AFM tip retraction (found at 37 °C) is abolished. The result strongly indicates that there is negligible adhesion between the AFM tip

and the polymer film. The indifference between the approach and retraction regimes on the force curve as mentioned above is similar to that of a bare glass substrate [11]. The result is likely caused by the change of hydrophilicity of the polymer film or the desorption of the polymer from the substrate into the aqueous medium below LCST.

The structural transition of HBC29 film as mentioned above likely alters the thermal-induced response of adherent cell. Fig. 3 shows a series of (a) phase contrast images and (b) C-RICM images of a typical SMC (pre-cultured for 3 h at 37 °C) on HBC29 surface during different times of 18 °C incubation. After 5 min of low-temperature incubation, the phase contrast image demonstrates that the cell expresses an elongated morphology with a projected area of 295.2 μm^2. From C-RICM image, it is shown that the initial adhesion contact has an area of 179.9 μm^2. Our result validates that HBC29 is biocompatible for SMC compared to unmodified TCPS. From 5 to 10 min, it is shown that the adhesion contact acutely recedes (arrowhead on C-RICM image) in parallel with the retraction of the lamellipodium at the bottom half of the cell body (arrowhead on phase contrast image). During the period, the cell transforms from an elongated to round geometry. At 10 min, the projected area and adhesion contact area is 164.9 and 120.8 μm^2, respectively. From 10 to 20 min, the adhesion contact area is further reduced to 84.8 μm^2, while the projected area remains constant. From 20 to 60 min, the cell remains round in shape without any lamellipodium formation and shows further reduction in adhesion contact area from 84.8 to 36.1 μm^2. Overall, the adhesion contact area and projected area is reduced by 80% and 82%, respectively. The result also indicates that cell retraction roughly synergizes with the adhesion contact recession.

It has been recently shown that the increase of RMS roughness of polymeric biomaterial surface directly promotes cell adhesion without any alteration of the biomaterial's bulk properties [28]. The previous result as mentioned above agrees well with our data herein on the stronger cell adhesion on the rougher HBC29 surface above LCST compared with that on the smoother surface below LCST based on our AFM data. Therefore, the cell deadhesion is partially triggered by the significant reduction of RMS roughness on the HBC29 surface. Alternatively, the surface chemistry of biomaterial surface is directly reflected by the static contact angle [12]. The static contact angle of HBC29 surface is 30.1±3.3° and 15.7±1.1° at 22 and 37 °C, respectively. As a result, the change in surface chemistry of the HBC29 polymer across LCST also plays an important role in the thermal-induced responses of adherent cells. The lack of complete cell detachment during low-temperature incubation is likely linked to the presence of serum proteins, which replenish the desorbed ECM proteins on HBC 29 surface during low-temperature incubation.

The change of pre-culture time on TRP affects the thermal-induced responses of SMC. Fig. 4 shows a series of (a) phase contrast images and (b) C-RICM images of a typical SMC (pre-cultured for 9 h at 37 °C) on HBC29 surface at different time points during the 18 °C incubation. After 5 min, the cell maintains an elongated morphology with a projected area and adhesion contact area of 669.1 and 345.4 μm^2, respectively. From 5 to 10 min, the lamellipodium at the bottom cell body slightly retracts upward (projected area: 559.1 μm^2), follows by slower recession of adhesion contact (with area of 335.7 μm^2) in comparison with cell pre-cultured for 3 h. From 10 to 20 min, phase contrast image shows that the lamellipodium significantly reduces in size (projected area of cell: 226.6 μm^2) and fails to form any adhesion contact (contact area of cell: 124.7 μm^2). At 20 min, the relative length of the lamellipodium of the cell pre-cultured for 9 h (aspect ratio: 3.33) is significantly longer than that of cell pre-cultured for 3 h (aspect ratio: 1.42). From 20 min onward, the cell continues to transform from elongated to elliptical shape until the lamellipodium disappears at 60 min. Overall, the projected area and adhesion contact area is reduced by 75% and 70%, respectively. Generally, the increase of pre-culture time leads to a change of cell deadhesion mechanism on HBC29 surface, e.g., delay in adhesion contact recession.

Fig. 5 shows a series of (a) phase contrast images and (b) C-RICM images for a typical SMC on HBC29 surface, which has been pre-cultured for 24 h (at 37 °C) and then incubated at 18 °C. After 5 min, phase contract image indicates the cell is highly elongated and forms highly extended lamellipodium. Also, the projected area and adhesion contact area is 921.2 and 593.7 μm^2, respectively. From 5 to 20 min, the cell moderately retracts (projected area: 771.4 μm^2) and reduces in strong adhesion contact (with area of 492.7 μm^2) in contrast to the rapid retraction found in cell pre-cultured for 3 h at 37 °C. Interestingly, the relative length of the lamellipodium at 20 min is highest (aspect ratio: 4.3) among cells under different pre-culture times. From 20 to 30 min, the cell significantly retracts (projected area reduces from 771.4 to 379.1 μm^2) and transform from an elongated to elliptical geometry. Also, the abrupt retraction is concurrent with the recession of adhesion contact (area reduces from 492.7 to 272.4 μm^2). After 60 min, thin lamellipodium, which is not found in cell pre-cultured for 3 or 9 h remains on the cell body. Overall, the projected area and adhesion contact is reduced by 63% and 62%, respectively. Interestingly, the trend as mentioned above indicates that further increase of pre-culture time significantly delays the retraction and deadhesion of cell on HBC 29 surface. Our results herein have not demonstrated the migration and complete detachment of cells like BAECs on PIPAAm surface [12]. It is because the physiochemical properties of HBC29 are different from those of PIPAAM. Moreover, the SMC chosen in our study is different from BAECs. The exact difference in the mechanisms of thermal-induced responses between our HBC29 system and PIPAAm system needs to be further clarified by future biophysical investigations.

In this study, we aim to quantify the effect of thermal transition of TRP on the cell–substrate interaction. Therefore, the normalized adhesion contact area which is defined as the ratio between the initial adhesion contact area (A_0) and adhesion contact area at anytime during the low-temperature incubation (A) is used herein. Similar parameter has been used for analyzing the growth of adhesion contact area during cell seeding [19]. Fig. 6A shows the average A/A_0 for SMCs pre-incubated for 3, 9 and 24 h against time of low-temperature incubation at 18 °C. The error bar is the standard error of at least 80 cells on five identical samples. In general, A/A_0 follows the trend of double exponential decay against time until it reaches a steady-state level despite the change of pre-culture time. The reduction of A/A_0 is faster at the early stage of cell deadhesion due to the acute retraction of cell bodies and loss in adhesion contact as mentioned above. By fitting the experimental data with the typical exponential decay function, $Y = (1-a)+ae^{-bx}$, the kinetic coefficients a and b are obtained (Table 1). The resulted fittings of the experimental data capture both the fast decay of A/A_0 at earlier time point and the reaching of steady state towards the later time point. It is determined that the steady-state value of A/A_0 which is equal to $(1-a)$ for cell pre-cultured at 3, 9 and 24 h is 0.31, 0.47 and 0.46, respectively. Moreover, b for cells pre-cultured at 3, 9 and 24 h is 0.0401, 0.0377 and 0.0288 h^{-1}, respectively. The result indicates that initial rate of A/A_0 reduction is highest for cells, which are pre-cultured for 3 h at 37 °C. Moreover, the increase of pre-culture time leads to significant reduction of b by 6% and 28% in cells pre-cultured for 9 and 24 h, respectively. The trend of b as mentioned above is likely caused by the stronger anchorage formed by SMCs with HBC29 surface against the increase of pre-culture time at the physiological temperature.

Several biological functions including cell fusion, proliferation and differentiation are induced by cell deformation upon adhesive interactions on ECM or biomaterials. So far, the kinetics of adhesion contact recession for SMC on HBC 29 during the thermal-induced process is elucidated. However, the change of A/A_0 is not directly related to the geometric transformation of the cell during the reduction of cell–substrate contact. To quantify the change of geometry of SMC, a biophysical parameter known as the degree of cell deformation (a/R) plays a crucial role [8]. Fig. 6B shows the average a/R for SMCs pre-incubated for 3, 9 and 24 h (at 37 °C) against time during low-temperature incubation at 18 °C. The error bar represents the standard error of at least 80 cells on five identical samples. The result indicates that average a/R for cells

pre-cultured on HBC29 for 9 and 24 h remains constant at around 0.78 and 0.81, respectively, during 150 min of low-temperature incubation. The constant value of a/R as mentioned above indicates that the cell projection and adhesion contact simultaneously recede against time. In contrast, cells pre-cultured for 3 h demonstrate a significant reduction of average a/R from 0.8 to 0.65 as the time of low-temperature incubation increases from 15 to 150 min. The result strongly indicates that the reduction of pre-culture time demolishes the synergy between adhesion contact recession and cell retraction. Specifically, the higher rate of adhesion contact recession in comparison with cell body retraction would trigger the detachment of cell from the substrate. In the current study, the use of a/R (directly determined from the ratio of adhesion contact area and projected area) should be applicable for the interpretation of the geometry transformation of elliptical cells (Wan KT, personal communication).

Average adhesion energy is directly correlated with the degree of deformation and mechanical properties of cell as shown in our contact mechanics model [8]. Fig. 7A shows the average adhesion energy for SMCs pre-cultured for 3, 9 and 24 h against time during low-temperature incubation at 18 °C. The error bar is the standard error of at least 80 cells on five identical samples. The result shows that the average adhesion energy of cells pre-cultured for 9 and 24 h stays constant at around 1.14×10^{-7} and 1.39×10^{-7} J/m^2, respectively, from 5 to 120 min after low-temperature incubation. The trend as mentioned above may still imply a change on the adhesion strength between cell and substrate because the adhesion energy unit is normalized with adhesion contact area, which is a reducing function of time. In contrast, average adhesion energy of cells pre-cultured for 3 h is steadily reduced from 1.33×10^{-7} to 3.33×10^{-8} J/m^2 (by four times) from 5 to 150 min of low-temperature incubation. The result strongly supports that the pre-culture time directly influences the temporal trend of average adhesion energy during cell deadhesion on TRP below LCST.

The adhesion energy per cell is defined as the product of average adhesion energy and adhesion contact area. Fig. 7B shows the adhesion energy per cell for SMCs pre-incubated for 3, 9 and 24 h against time during low-temperature incubation at 18 °C. The error bar is the standard error of at least 80 cells on five identical samples. The result shows that the adhesion energy per cell of SMCs pre-cultured for 9 and 24 h is reduced from 3.81×10^{-17} to 1.85×10^{-17} J (by 2 times) and 5.36×10^{-17} to 3.82×10^{-17} J (by 1.4 times), respectively, from 5 to 150 min after 18 °C incubation. The trend as mentioned above is different from that of the average adhesion energy because the adhesion energy per cell takes the change of adhesion contact area against time into consideration. Moreover, the extent in the reduction of adhesion energy per cell from 4.72×10^{-17} to 5.27×10^{-18} J (by 9 times) is highest on cell pre-cultured for 3 h. Overall, the result strongly indicates that the adhesive interaction between individual cells and HBC29 surface is reduced for all three types of cells and the extent of reduction in adhesion energy per cell is negatively correlated with the pre-culture time. In general, the biophysical responses of single cell on HBC29 as reported herein may not directly correlate with those of cell sheet. In a recent study, a group has demonstrated that either decreasing substratum adhesivity or increasing cell–cell cohesiveness dramatically slowed the spreading rate of cell aggregates on biomaterial surface [29]. In detail, cell–cell adhesion counterbalances the cell–substrate adhesion and moderates the rate of cell spreading upon the initial seeding of cells on biomaterials. Therefore, we hypothesize that the development of intercellular contacts in cell sheet will likely reduce the cell–substrate adhesion and eventually increases the rate of cell deadhesion from TRP. The detailed effect of cell–cell adhesion on the cell deadhesion dynamics will be focused in our future study.

In response to environmental cues, an anchorage-dependent cell changes both its shape and its extent of attachment to substratum through the rearrangement of cytoskeleton. For instance, F-actin, which is a major component of cytoskeleton induces filopodia formation in the plasma membrane during cell spreading and migration [14]. It is important to correlate the kinetics of

thermal-induced deadhesion with the cytoskeleton remodeling of SMCs on TRP. Fig. 8A shows the immuno-fluorescence image of a typical SMC (pre-cultured for 3 h at 37 °C) after 2, 30, and 60 min of low-temperature incubation at 18 °C. The scale-bar represents 10 μm. After 2 min, the result indicates that actin concentrates at the front of lamellipodia of the elongated SMC. There is also sign of microfilament formation in the cytoplasm of the cell. The presence of actin in a parallel filamentous array suggests the development of a contractile structure, which is the characteristic phenotype of contractile SMC [15]. The result supports the notion that the cytoskeleton organization of SMC on HBC29 remains intact during the early stage of thermal-induced deadhesion. From 2 to 30 min after low-temperature incubation, the actin further concentrates at cell periphery during the significant retraction of the cell. Also, the characteristic morphology of contractile SMC is lost. After 60 min of low-temperature incubation, further recession of the actin ring at cell periphery, which coincides with the reduction of adhesion contact area is detected.

The effect of pre-culture time may affect the cytoskeleton organization during cell deadhesion on TRP. Similar to cell pre-cultured for 3 h, actin concentrates at the lamellipodia of SMC pre-cultured for 9 h during the first 2 min of 18 °C incubation (Fig. 8B). At the same time, parallel actin microfilaments are found in the cytoplasm of the cell. From 5 to 30 min, cell retraction has led to an increase of actin concentration at cell periphery. At the same time, an intense microfilament is formed in the middle of the cell body during the transformation from elongated to elliptical shape. Interestingly, the typical contractile phenotype of SMC at 30 min is more obvious than that of the cell pre-cultured for 3 h. After 60 min of low-temperature incubation, higher concentration of actin is detected at the lamellipodium, which is the active site of mechanochemical transduction during cell deadhesion in comparison with the cell pre-cultured for 3 h. For cell pre-cultured for 24 h, the cell demonstrates highly elongated morphology after 2 min of low-temperature incubation and is accompanied by the formation of filpodia (arrows) with high actin concentration (Fig. 8C). Moreover, the cell still maintains the more convoluted shape (arrows) as outlined by the actin distribution at the filopodia after 30 min in contrast to cells with less pre-culture time. Finally, the cell retraction from 30 to 60 min leads to the formation of circular ring of actin at cell periphery. However, the convoluted extensions and filopodia, which are not found in cells with lower incubation time remains after 60 min. The result suggests that the increase of pre-culture time will resist the fading of filopodia during cell deadhesion. Therefore, cytoskeleton transformation during low-temperature incubation is correlated with the deadhesion dynamics of cells on HBC29. Taken together, the result reported herein on cytoskeleton organization is in accord with the result from the harvest of BAECs cell sheet on TRP. For BAECs cell sheet detachment, the peripheral ring composed of actin filaments are also preserved during the shrinking of the whole cell sheet [16].

Actin is a ubiquitous protein present in large amounts in all cells and tissues. For SMC, actin is distributed uniformly within the cell. In the actin family, β-actin is a cytoskeletal protein and induces the formation of micro-filaments and stress fibers that influence the cytoarchitecture of the cell. In vascular SMC, β-actin rather than alpha-actin expression becomes dominant, particularly when SMC undergoes phenotypic modulation [17]. During canine myocardium vascular remodeling, β-actin mRNA is upregulated in transmyocardial by direct-current shock treatment [18]. Therefore, β-actin gene expression has served as a key functional marker for phenotypic modulation of SMC and vascular remodeling.

Fig. 9A shows the temporal trend of mRNA expression of β-actin during 18 °C incubation for cell pre-cultured at 37 °C for 3 h (lanes 2–4) and 24 h (lanes 5–7). After 30 min of incubation at 18 °C, the expression of β-actin mRNA of cells pre-cultured for 3 h is significantly reduced compared to cells before deadhesion at 37 °C. Towards 60 min of 18 °C incubation, the level of β-actin expression is unaltered compared to the cells subjected to 30 min of 18 °C incubation. This result is supported by the phase contrast images in Fig. 3. After 30 min of incubation at

18 °C, most cells change to round morphology and remain unaltered until 60 min of low-temperature incubation. For cells pre-cultured for 24 h, the expression of β-actin mRNA before the low-temperature incubation is significantly higher than that of cells pre-cultured for 3 h. The result is in accordance with the higher degree of cell spreading on the TRP surface induced by the increase of pre-culture time before the temperature drops below LCST. It is because cells synthesize more cytoskeletal β-actin when they are spreading and growing. After 30 min of 18 °C incubation, the level of β-actin expression remains high compared to that before cell deadhesion. The result is also supported by the reduction in the initial deadhesion rate in cells pre-cultured for 24 h (Fig. 5). After 60 min of incubation at 18 °C, the mRNA expression is significantly reduced to the level close to that of cells pre-cultured for 3 h. This result follows the trend of the cell morphology and adhesion data. For example, both the 3 h pre-cultured and 24 h pre-cultured cells shrink to a truncated sphere after 60 min of incubation at 18 °C.

Generally the SMCs can be divided into two phenotypes: proliferative (synthetic) and contractile phenotype. The commonly known marker proteins, such as smooth muscle heavy myosin, α-smooth muscle actin, vinculin/metavinculin, SM22, calponin and h-caldesmon have been used to understand the differentiation of SMC. But the specificity of these markers for a distinct phenotype is low since other cell types also express these marker proteins [20]. In contrast, smoothelin-B, a novel structural protein is only found in contractile SMCs. Cells with SMC-like characteristics, such as myofibroblasts, myoepithelial cells, skeletal and cardiac muscle do not contain smoothelin-B [21,22]. The expression of smoothelin-B would be stopped when a balloon injury is introduced to the rat carotid artery, which would lead to a dedifferentiation of the SMCs in neointima and media [23]. Also, the smoothelin-B shows the characteristic of co-localization with different isoforms of actin [24–25]. The co-localization of smoothelin-B with filamentous actin but not G-actin indicates its effect on actin filament rigidity or actin bundle stabilization.

In previous studies of chicken embryogenesis [24], it has been proven that smoothelin-B is expressed in all embryonic, neonatal and adult vascular SMC, which suggests that the contribution of this isoform to the biological functions of vascular SMC does not change during life. In another studies of normal human large muscular arteries, the immuno-fluorescence signals of smoothelin are higher than that of desmin while Western blot data show opposite trend [26]. As a result, we use RT-PCR, which is more sensitive than Western blot to detect the expression of smoothelin-B in SMC. Fig. 9B shows the time course of change in smoothelin-B mRNA expression during 18 °C incubation for cells pre-cultured at 37 °C for 3 h (lanes 2–4) and 24 h (lanes 5–7). For both kinds of cells, the positive expression of smoothelin-B indicates the cells tend to be contractile before the detachment. The 3 h pre-cultured cells express more smoothelin-B than 24 h pre-culture cells before the detachment process. The result implies that longer pre-culture time (24 h) may moderate the specific phenotype of SMCs, compared with a shorter pre-culture time (3 h). This possibility is supported by previous reports indicating that smoothelin-B expression decreases as the number of passages of cultured SMC cells increase [27]. For both types of cells, the expression of smoothelin-B hugely increases during the cell detachment process, which means the cells are modulated to a more contractile phenotype during this process. The main change as mentioned above appears after 30 min of incubation at 18 °C for 3 h pre-cultured cells and around 60 min for 24 h pre-cultured cells. This delay induce by the increase of pre-culture time proves that the temporal response of a typical SMC phenotype towards the thermal transition of TRP is directly correlated with the reduction in deadhesion rate of SMCs against the increase of pre-culture time.

It is commonly known that several physical and biological cues including ECM protein coating, serum protein, cell type, etc., directly affects the adhesion strength of anchorage-dependent cells on biomaterial surfaces during initial cell seeding [30]. In addition to the pre-culture time

of cell, it is likely that those physical and biological factors as mentioned above will influence the cell deadhesion dynamics and resulting cellular phenotypes of cells on HBC29 surface. For instance, our group has obtained preliminary data on the deadhesion dynamics of other cell types such as the primary human SMCs on the HBC29 surface. Our preliminary result shows that the general trend of cell deadhesion kinetics for primary SMC against the change of pre-culture time is similar to that of SMC cell line used herein. On the other hand, further in-depth study on the effect of those additional physical/biological factors as mentioned above on the cell deadhesion dynamics will deviate from our main objective in correlating the thermal-induced biophysical behavior of a model SMC with common cell phenotypes herein.

4. Conclusion

In summary, we have demonstrated the possibility of elucidating the cell deadhesion dynamics in order to control the cytoskeleton organization and specific phenotypes of SMCs on a model TRP. It is shown that several key biophysical parameters including normalized adhesion contact area, degree of deformation and adhesion energy per cell are correlated with the pre-culture time of SMC before low-temperature incubation. Lastly, the cytoskeleton remodeling as well as the mRNA expression of β-actin or smoothelin-B is correlated with the pre-culture time or deadhesion kinetics of SMC under different pre-culture times.

Acknowledgements

JD and KWL acknowledge the support of NIH (EB003447). BC and VC were supported by AcRF RG52/06.

References

1. Yamada N, Okuhara M, Sakai H, Sakurai Y, Okano T. Mechanism of cell detachment from temperature-modulated, hydrophilic-hydrophobic polymer surfaces. Biomaterials 1995;16(4):297–303. [PubMed: 7772669]
2. Kikuchi A, Okano T. Nanostructured designs of biomedical materials: applications of cell sheet engineering to functional regenerative tissues and organs. J Control Release 2005;101(1–3):69–84. [PubMed: 15588895]
3. Kushida A, Yamato M, Konno C, Kikuchi A, Okano T. Temperature-responsive culture dishes allow non-enzymatic harvest of differentiated Madin–Darby canine kidney(MDCK) cell sheets. J Biomed Mater Res 2000;51(2):216–23. [PubMed: 10825221]
4. Morikawa N, Matsuda T. Thermoresponsive artificial extracellular matrix: *N*-isopropylacrylamide-graft-copolymerized gelatin. J Biomater Sci Polym Ed 2002;13(2):167–83. [PubMed: 12022748]
5. Tan WJ, Teo GP, Liao K, Leong KW, Mao HQ, Chan V. Adhesion contact dynamics of primary hepatocytes on poly(ethylene terephthalate) surface. Biomaterials 2005;26(8):891–8. [PubMed: 15353200]
6. Dang JM, Sun DD, Shin-ya Y, Sieber AN, Kostuik JP, Leong KW. Temperature-responsive hydroxybutyl chitosan for the culture of mesenchymal stem cells and intervertebral disk cells. Biomaterials 2006;27(3):406–18. [PubMed: 16115680]
7. Yim EK, Reano RM, Pang SW, Yee AF, Chen CS, Leong KW. Nanopattern-induced changes in morphology and motility of smooth muscle cells. Biomaterials 2005;26(26):5405–13. [PubMed: 15814139]
8. Liu KK, Wan KT. Contact mechanics of a thin-walled capsule adhered onto a rigid planar substrate. Med Biol Eng Comput 2001;39(5):605–8. [PubMed: 11712660]
9. Nagayama K, Nagano Y, Sato M, Matsumoto T. Effect of actin filament distribution on tensile properties of smooth muscle cells obtained from rat thoracic aortas. J Biomech 2006;39(2):293–301. [PubMed: 16321631]
10. Bunnell BA, Muul LM, Donahue RE, Blaese RM, Morgan RA. High-efficiency retroviral-mediated gege-transfer into human and nonhuman primate peripheral-blood lymphocytes. Proc Natl Acad Sci 1995;92(17):7739–43. [PubMed: 7644487]

11. Li SL, Palmer AF. Structure and mechanical response of self-assembled poly(butadiene)-*b*-poly (ethylene oxide) colloids probed by atomic force microscopy. Macromolecules 2005;38(13):5686–98.
12. Plunkett NK, Zhu X, Moore JS, Leckband DE. PNIPAm chain collapse depends on the molecular weight and grafting density. Langmuir 2006;22(9):4259–66. [PubMed: 16618173]
13. Yin C, Liao K, Mao HQ, Leong KW, Zhuo RX, Chan V. Adhesion contact dynamics of HepG2 cells on galactose immobilized substrates. Biomaterials 2003;24(5):837–50. [PubMed: 12485802]
14. Ghosh M, Song X, Mouneimne G, Sidani M, Lawrence DS, Condeelis JS. Cofilin promotes actin polymerization and defines the direction of cell motility. Science 2004;304(5671):743–6. [PubMed: 15118165]
15. Niessen P, Clement S, Fontao L, Chaponnier C, Teunissen B, Rensen S, et al. Biochemical evidence for interaction between smoothelin and filamentous actin. Exp Cell Res 2004;292(1):170–8. [PubMed: 14720516]
16. Konno C, Kikuchi A, Sakurai Y, Okano T, Kushida A, Yamato M. Decrease in culture temperature releases monolayer endothelial cell sheets together with deposited fibronectin matrix from temperature-responsive culture surfaces. J Biomed Mater Res 1999;45(4):355–62. [PubMed: 10321708]
17. Etienne P, Pares Herbute N, Mani Ponset L, Gabrion J, Rabesandratana H, Herbute S, et al. Phenotype modulation in primary cultures of aortic smooth muscle cells from streptozotocin-diabetic ras. Differentiation 1998;63(4):225–36. [PubMed: 9745713]
18. Carlyle WC, Toher CA, Vandervelde JR, McDonald KM, Homans DC, Cohn JN. Changes in beta-actin mRNA expression in remodeling canine myocardium. J Mol Cell Cardiol 1996;28(1):53–63. [PubMed: 8745214]
19. Chamaraux F, Fache S, Bruckert F, Fourcade B. Kinetics of cell spreading. Phys Rev Lett 2005;94:158102. [PubMed: 15904192]
20. Owens GK. Regulation of differentiation of vascular smooth muscle cells. Physiol Rev 1995;75:487–517. [PubMed: 7624392]
21. van Eys, GJJM.; de Vries, CJM.; Rensen, SSM.; Thijssen, VLJL.; Verkaar, ELC.; Coolen, GPGM., et al. Smoothelins: one gene, two proteins, three muscle cell types… so far. In: Doevendans, PA., editor. Cardiovascular specific gene expression. Dordrecht: Kluwer Academic Publishing; 1999. p. 49-63.
22. Bar H, Wende P, Watson L, Denger S, van Eys G, Kreuzer J, et al. Smoothelin is an indicator of reversible phenotype modulation of smooth muscle cells in balloon-injured rat carotid arteries. Basic Res Cardiol 2002;97(1):9–16. [PubMed: 11998981]
23. Christen T, Bochaton-Piallat ML, Neuville P, Rensen S, Redard M, van Eys G, et al. Cultured porcine coronary artery smooth muscle cells (a new model with advanced differentiation). Circ Res 1999;85:99–107. [PubMed: 10400915]
24. Deruiter MC, Rensen SS, Coolen GP, Hierck BP, Bergwerff M, Debie WM, et al. Smoothelin expression during chicken embryogenesis: detection of an embryonic isofrom. Dev Dyn 2001;221:460–3. [PubMed: 11500983]
25. Niessen P, Clement S, Fontao L, Chaponnier C, Teunissen B, Rensen S, et al. Biochemical evidence for interaction between smoothelin and filamentous actin. Exp cell Res 2004;292(1):170–8. [PubMed: 14720516]
26. Van der Loop FT, Gabbiani G, Kohnen G, Ramaekers FC, Van Eys GJ. Differentiation of smooth muscle cells in human blood vessels as defined by smoothelin, a novel marker for the contractile phenotype. Arter Throm Vas Bio 1997;17(4):665–71.
27. Van der Loop FT, Schaart G, Timmer ED, Ramaekers FC, Van Eys GJ. Smoothelin, a novel cytoskeletal protein specific for smooth muscle cells. J Cell Biol 1996;134(2):401–11. [PubMed: 8707825]
28. Sannino A, Conversano F, Esposito A, Maffezzoli A. Polymeric meshes for internal sutures with differentiated adhesion on the two sides. J Mater Sci Mater Med 2005;16(4):289–96. [PubMed: 15803272]

29. Ryan PL, Foty RA, Kohn J, Steinberg MS. Tissue spreading on implantable substrates is a competitive outcome of cell-cell vs. cell-substratum adhesivity. Proc Natl Acad Sci USA 2001;98(8):4323–7. [PubMed: 11274361]

30. Lord MS, Modin C, Foss M, Duch M, Simmons A, Pedersen FS, et al. Monitoring cell adhesion on tantalum and oxidised polystyrene using a quartz crystal microbalance with dissipation. Biomaterials 2006;27(26):4529–37. [PubMed: 16716396]

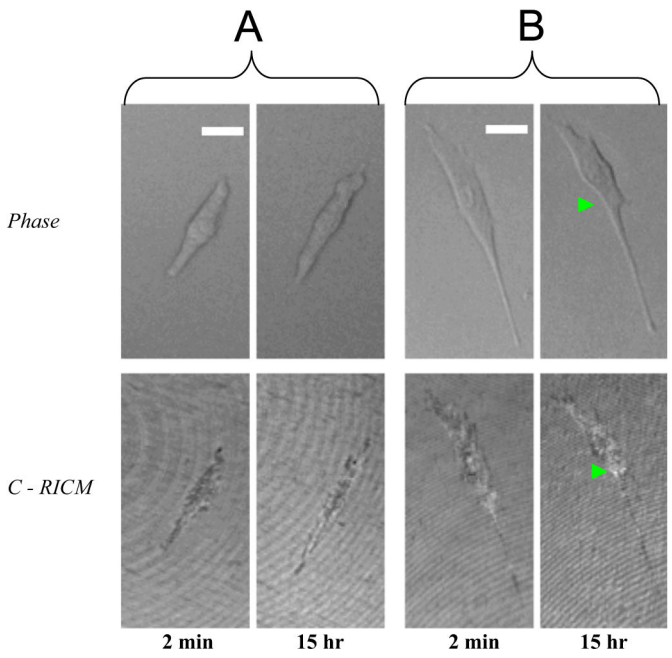

Fig. 1.

The real-time phase contrast images and C-RICM images of a typical SMC pre-cultured for (A) 3 h and (B) 24 h at 37 °C and 5% CO_2 on untreated TCPS surfaces after 2 min and 15 h of incubation at 18 °C and 5% CO_2. The scale bar represents 10 μm.

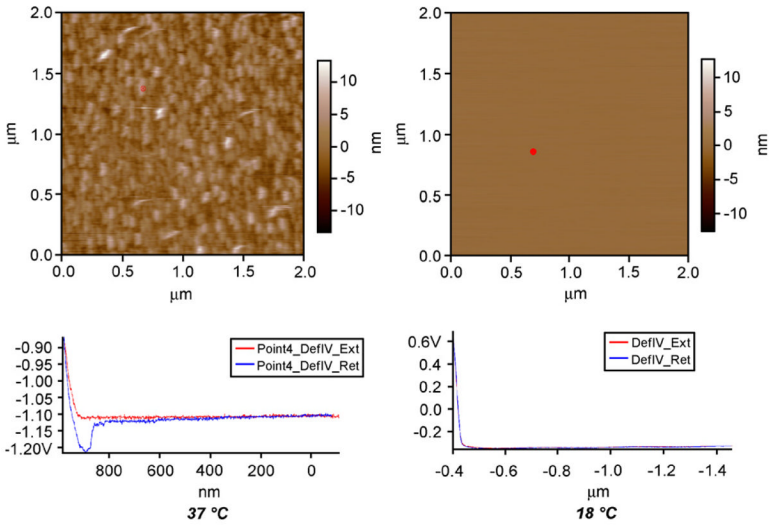

Fig. 2.

AFM topographic images of HBC29 film immersed in pure water at 37 and 18 °C.

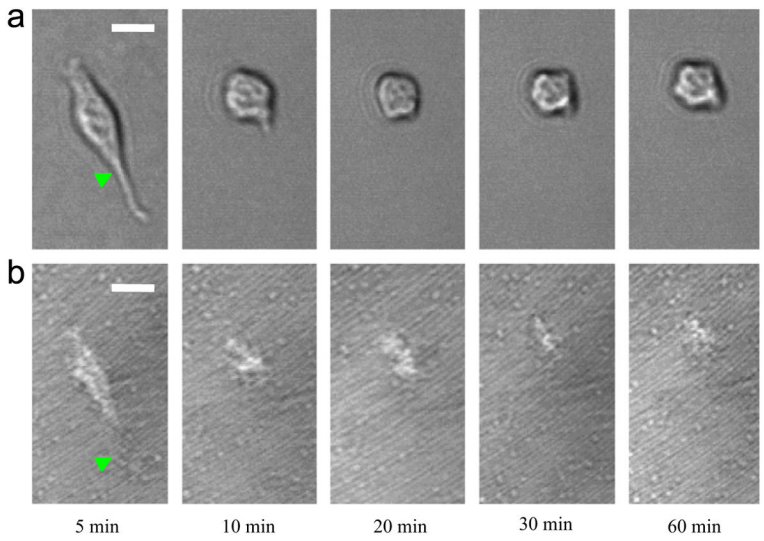

Fig. 3.

A series of (a) phase contrast images and (b) C-RICM images for a typical SMC on HBC 29 surface, which has been pre-cultured at 37 °C for 3 h at different times during 18 °C incubation. The scale-bar represents 10 μm.

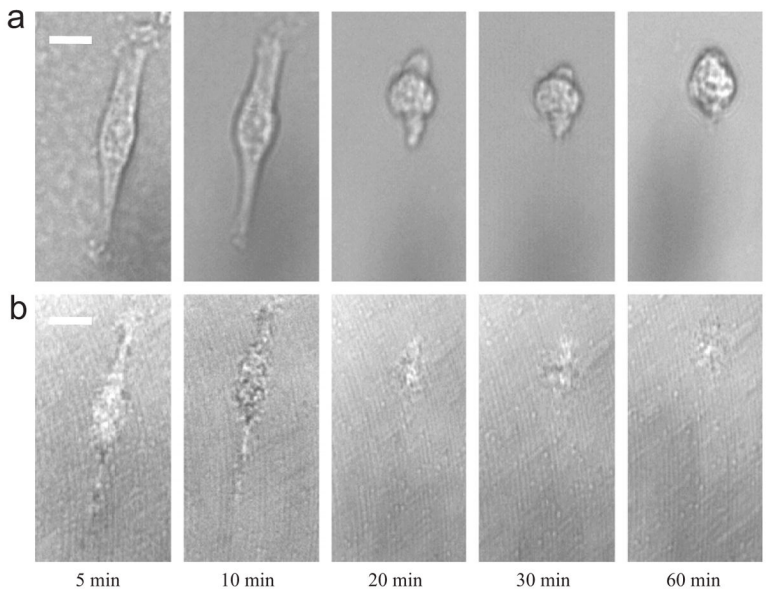

Fig. 4.

A series of (a) phase contrast images and (b) C-RICM images for a typical SMC on HBC 29 surface, which has been pre-cultured at 37 °C for 9 h at different times during 18 °C incubation. The scale-bar represents 10 μm.

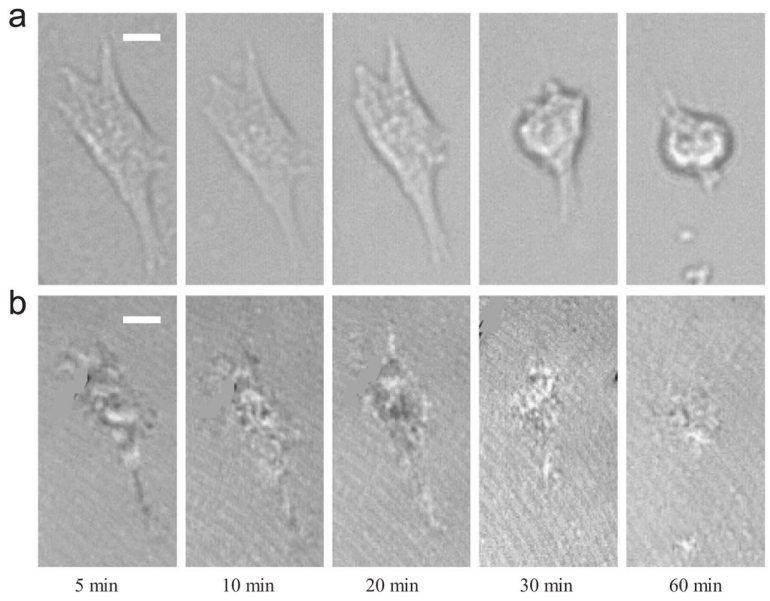

Fig. 5.

A series of (a) phase contrast images and (b) C-RICM images for a typical SMC on HBC 29 surface which has been pre-cultured at 37 °C for 24 h at different times during low-temperature (18 °C) incubation under 5% CO_2. The scale-bar represents 10 μm.

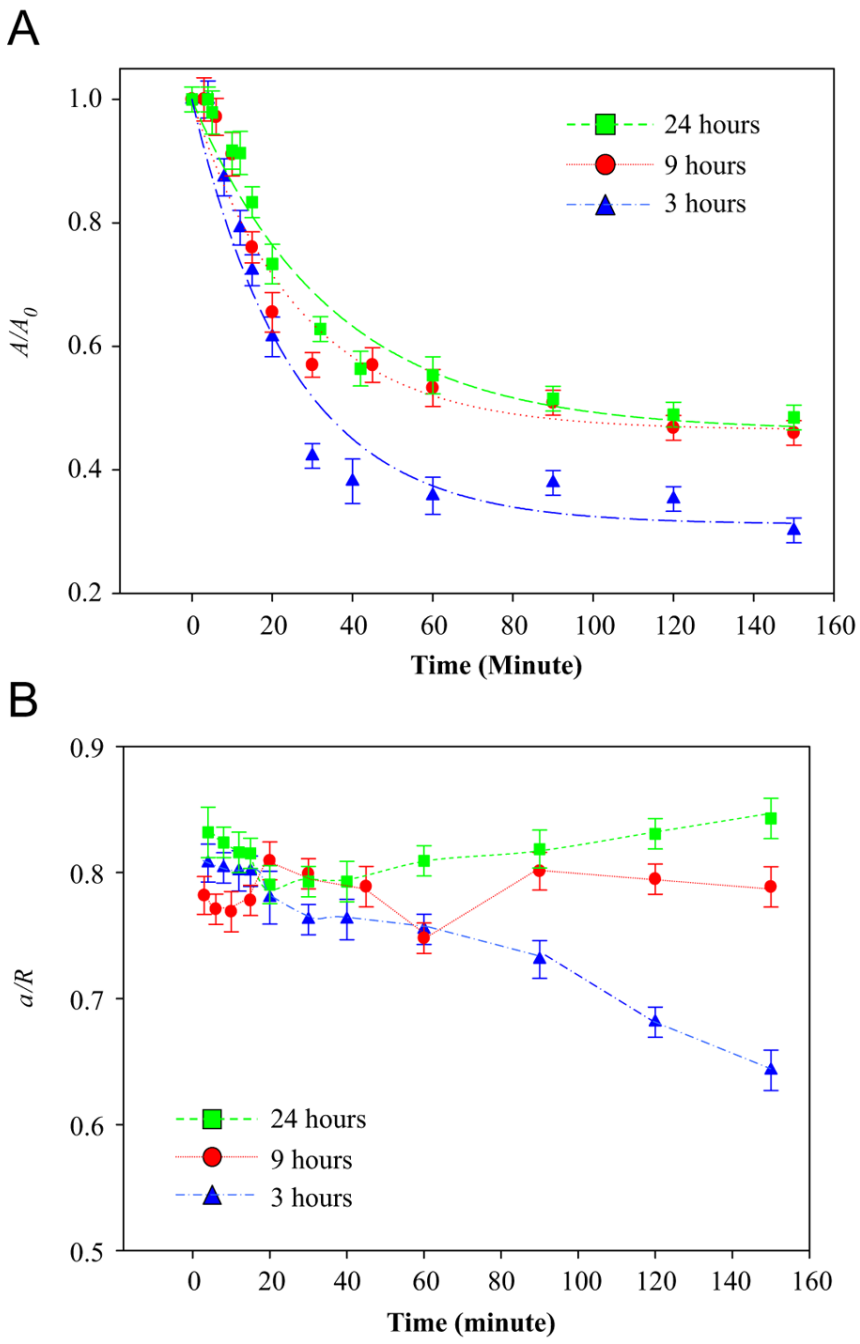

Fig. 6.

(A) Average A/A_0 for SMCs pre-incubated for 3, 9 and 24 h against time during low-temperature incubation at 18 °C. The error bar is the standard error of at least 80 cells on five identical samples. (B) The average a/R for SMCs pre-incubated for 3, 9 and 24 h against time during low-temperature incubation at 18 °C. The error bar is the standard error of at least 80 cells on five identical samples.

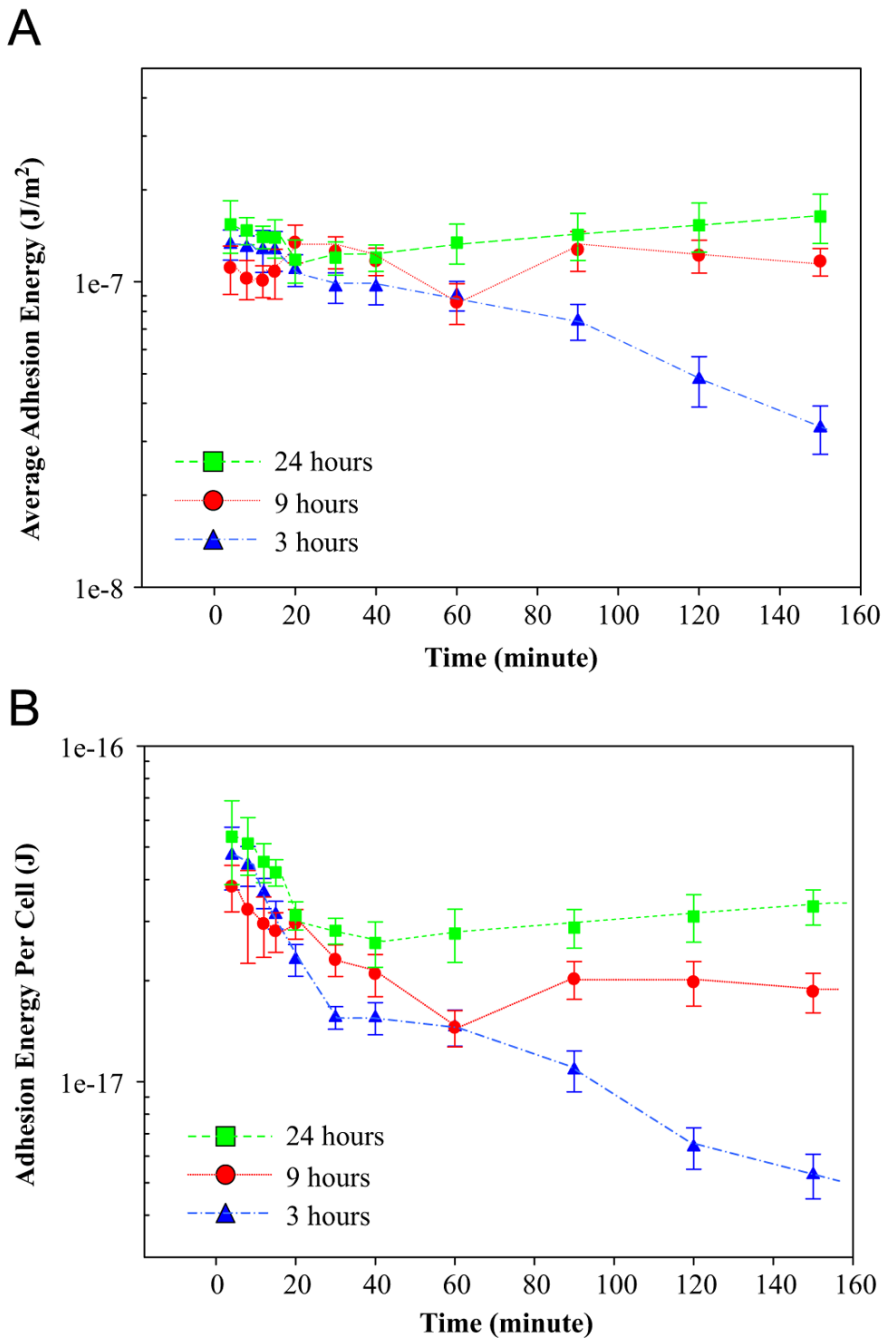

Fig. 7.

(A) The average adhesion energy for SMCs pre-incubated for 3, 9 and 24 h against time during low-temperature incubation at 18 °C. The error bar is the standard error of at least 80 cells on five identical samples. (B) The adhesion energy per cell for SMCs pre-incubated for 3, 9 and 24 h against time during low-temperature incubation at 18 °C. The error bar is the standard error of at least 80 cells on five identical samples.

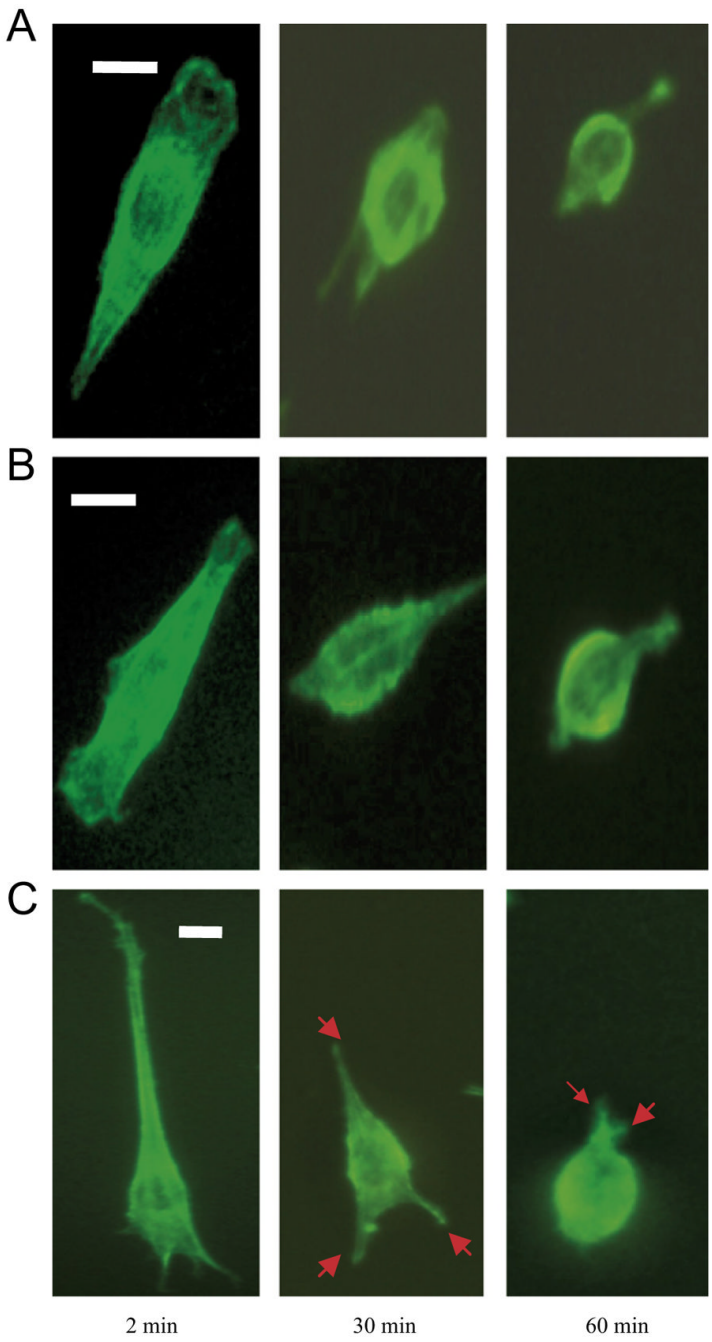

Fig. 8.
The fluorescence image of a typical SMC (actin staining) pre-cultured for (A) 3 h, (B) 9 h and (C) 24 h at 37 °C at 2, 30, and 60 min after low-temperature incubation at 18 °C. The scale-bar represents 10 μm.

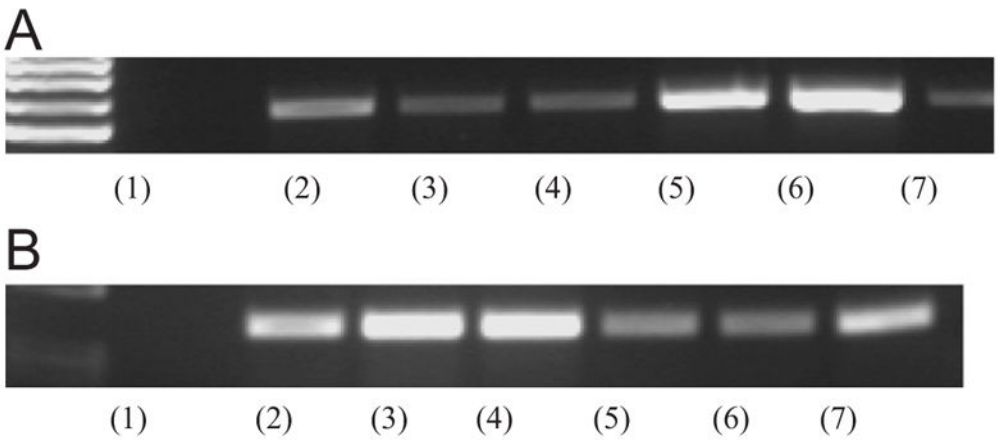

Fig. 9.

(A) The *β*-actin RT-PCR products arisen from the amplification of mRNA extracted from detaching A7r5 smooth muscle cells on HBC29 surface. Lane 1 shows the negative control. Lane 2 shows the *β*-actin expression for 3 h pre-cultured cells (at 37 °C) after 0 h of 18 °C incubation. Lane 3 shows the data for 3 h pre-cultured cells (at 37 °C) after 0.5 h of 18°C incubation. Lane 4 shows the data for 3 h pre-cultured cells (at 37 °C) after 1 h of 18 °C incubation. Lane 5 the *β*-actin expression for 24 h pre-cultured cells (at 37 °C) after 0 h of 18 °C incubation. Lane 6 the data for 24 h pre-cultured cells (at 37 °C) after 0.5 h of 18 °C incubation. Lane 7 shows the data for 24 h pre-cultured cells (at 37 °C) after 1 h of 18 °C incubation. (B) The smoothelin-B RT-PCR products arisen from the amplification of mRNA extracted from A7r5 smooth muscle cells on HBC29 surface. Lane 1 shows the negative control. Lane 2 shows the smoothelin-B expression for 3 h pre-cultured cells (at 37 °C) after 0 h of 18°C incubation. Lane 3 shows the data for 3 h pre-cultured cells (at 37 °C) after 0.5 hra of 18 °C incubation. Lane 4 shows the data for 3 h pre-cultured cells (at 37 °C) after 1 h of 18 °C incubation. Lane 5 the *β*-actin expression for 24 h pre-cultured cells (at 37 °C) after 0 h of 18 °C incubation. Lane 6 the data for 24 h pre-cultured cells (at 37 °C) after 0.5 h of 18 °C incubation. Lane 7 shows the data for 24 h pre-cultured cells (at 37 °C) after 1 h of 18 °C incubation.

Table 1

Fitted parameters in the deadhesion kinetics of smooth muscle cells on HBC 29

Culture Time (h)	*a*	*b*
24	0.54	0.0288
9	0.535	0.0377
3	0.688	0.0401